



HAL
open science

Full-scale tunnel experiments for hydrogen fuel cell vehicles: gas dispersion

Didier Bouix, François Sauzedde, Philippe Manicardi, Maximilien Martin, Diana Forero, Etienne Studer, Sergey Kudriakov, Gilles Bernard-Michel, Herve Gueguen

► **To cite this version:**

Didier Bouix, François Sauzedde, Philippe Manicardi, Maximilien Martin, Diana Forero, et al.. Full-scale tunnel experiments for hydrogen fuel cell vehicles: gas dispersion. ICHS - INTERNATIONAL CONFERENCE ON HYDROGEN SAFETY 2021, Sep 2021, Edimbourg, United Kingdom. cea-03777096

HAL Id: cea-03777096

<https://cea.hal.science/cea-03777096>

Submitted on 14 Sep 2022

HAL is a multi-disciplinary open access archive for the deposit and dissemination of scientific research documents, whether they are published or not. The documents may come from teaching and research institutions in France or abroad, or from public or private research centers.

L'archive ouverte pluridisciplinaire **HAL**, est destinée au dépôt et à la diffusion de documents scientifiques de niveau recherche, publiés ou non, émanant des établissements d'enseignement et de recherche français ou étrangers, des laboratoires publics ou privés.

FULL-SCALE TUNNEL EXPERIMENTS FOR FUEL CELL HYDROGEN VEHICLES: GAS DISPERSION

BOUIX D.¹, SAUZEDDE F.¹, MANICARDI P.¹, MARTIN M.¹,
FORERO D.², STUDER E.², BERNARD-MICHEL G.², KOUDRIAKOV S.², GUEGUEN H.²

¹ *Univ Grenoble Alpes, CEA, LITEN, DEHT, LSP, F-38000 Grenoble, , France*

² *DES, CEA, Université Paris-Saclay, Saclay, France.*

ABSTRACT

In the framework of the HYTUNNEL-CS European project sponsored by FCH-JU, a set of preliminary tests were conducted in a real tunnel in France. These tests are devoted to safety of hydrogen-fueled vehicles having a compressed gas storage and Temperature Pressure Release Device (TPRD). The goal of the study is to develop recommendations for Regulations, Codes and Standards (RCS) for inherently safer use of hydrogen vehicles in enclosed transportation systems. In these preliminary tests, the helium gas has been employed instead of hydrogen. Upward and downward gas releases following by TPRD activation, has been considered. The experimental data describing local behavior (close to jet or below the chassis) as well as global behavior at the tunnel scale are obtained. These experimental data are systematically compared to existing engineering correlations. The results will be used for benchmarking studies using CFD codes. The hydrogen pressure range in these preliminary tests has been lowered down to 20MPa in order to verify the capability of various large-scale measurement techniques before scaling up to 70MPa, the subject of the second campaign.

1.0 INTRODUCTION

Hydrogen Fuel Cell Electric Vehicles (HFC EVs) represent an alternative to replace current internal combustion engine vehicles. The use of these vehicles with storage of compressed gaseous hydrogen (CGH₂) or cryogenic liquid hydrogen (LH₂) in confined spaces, such as tunnels, underground car parks, etc., creates new challenges to ensure the protection of people and property and to keep the risk at an acceptable level. Several studies have shown that confinement or congestion can lead to severe accidental consequences compared to accidents in an open atmosphere. It is therefore necessary to develop validated hazard and risk assessment tools for the behavior of hydrogen in tunnels. The HYTUNNEL-CS project sponsored by the FCH-JU pursues this objective. Among the experiments carried out in support of the validation, the CEA is conducting full-scale tests in a road tunnel.

In the past, hydrogen gas releases in a tunnel-like geometry have been carried out by SRI at the Corral Hollow Experiment Site [1]. This is a scaled-down facility. The tube representing the tunnel is 78.5 m long and has a diameter of 2.4 m. It has an embankment in the lower part, which gives it a horseshoe shaped cross-section of 3.74 m². Sato et al. [2] describe hydrogen release experiments in this facility for cars or buses but also to leaks on bottled hydrogen transports. The releases are carried out through a tube placed 15cm above the road and oriented upwards. The scenarios were scaled using the method described by Hall et al. The hydrogen concentrations measured showed a maximum concentration of hydrogen directly above the point of release whether or not there was ventilation. This was probably due to the inertial effect of the jet, which is dominant for an upward discharge. Moving away from the nozzle, the hydrogen concentration decreased rapidly. Ventilation can greatly reduce the hydrogen concentration when the discharges are less inertial. All release scenarios studied lead to lean mixtures and maximum concentrations of 9 vol%. More recently, Houf et al. [1] describe experiments carried out in the same facility but for a simultaneous opening of three TPRDs under a vehicle. Leading to very high hydrogen concentrations, reaching up to 40% hydrogen volume near the ceiling at the discharge location and a concentration close to stoichiometry at 3m downstream of the release. Under the chassis, concentrations close to 100% are measured. Simulations carried out with the FLACS code confirm these values. Many other numerical simulations are available in the literature i.e. Venetsanos et al. [3], Middha et al. [4], Bie et al. [5] and Li et al [6]. Restricting ourselves to scenarios involving cars with a 700 bar pressure tank without ventilation (worst case), Venetsanos et al.

obtain a maximum flammable volume of 519 m³ (3.7 kg of hydrogen) for a release by a 6 mm TPRD approximately 20 seconds after the start of the release. Middha et al. calculate a maximum flammable volume of 270 m³ (1.33 kg) if the 4 mm TPRD releases downwards and 280 m³ (1.14 kg) if it releases upwards. For Houf et al, the simultaneous opening of three TPRDs leads to a maximum flammable volume of between 390 and 450 m³ depending on the ventilation rate chosen and this maximum is reached between 10 and 20 seconds after the start of the release. Finally, Li et al. present a release calculation with a TPRD of 2.25 mm upwards and obtain 16 seconds after the start of the release a sensible volume (layered TDD criterion) of approximately 72 m³ for a mass of 2.9 kg of hydrogen. We conclude that in all these cases, there is limited number of experimental data for model validation and especially no full-scale data.

The present article was sought to evaluate the dispersion that would take place in a tunnel using instead of hydrogen a not flammable gas as Helium. Many experiments in the literature as J. He et al [7], A. Prabhakar et al [8], shows numerical approaches in hydrogen safety studies by using helium measurements for hydrogen dispersion analysis. The first part of this article is devoted to the description of the geometry of the tunnel and the system used to simulate the HFC-EV. Then, the measurement devices are detailed in order to follow the tank blowdown transient and the gas mixing in the tunnel. The third part provides details of the results and gives some comparisons with simulation results. Conclusions follow. The article only takes into account the pre-tests carried out with a maximum pressure inside the cylinder of 200 bar but a second campaign with a maximum pressure of 700 bar is to be carried out in June 2021 and the main results will be added for the presentation at the conference.

2.0 GEOMETRY, MEASUREMENTS AND TEST SEQUENCES

2.1 TUNNEL GEOMETRY AND GAS RELEASE DEVICE

The experiments were carried out in the Tunnel du Mortier located in the commune of Autrans in the Vercors, France (Figure 1) with the support of the council area of Isere Department. This tunnel is 502m long and is a disused straight road tunnel in the shape of a horseshoe. On the entrance (On Autrans side) the vault is concreted (images 1 and 2) while the inside of the tunnel is in rough rock (images 3 and 4). The concrete section is 133m long, 7.5m wide and 5.2m high. The rocky area represents the rest of the length with a width of 8.9m and a height of 5.6m. The slope is 3.6% and there is no mechanical ventilation. Finally, another concrete section is located at the exit of the tunnel (On Montaud side).

The tests were conducted 72m from the entrance to the concrete section. Two straw walls were installed at each end of the tunnel to limit natural convection, which could vary greatly from one day to the next depending on weather conditions. Under these conditions, the tests were practically all carried out with a wind speed inside the tunnel of about 0.3-0.4 m/s from top to bottom.

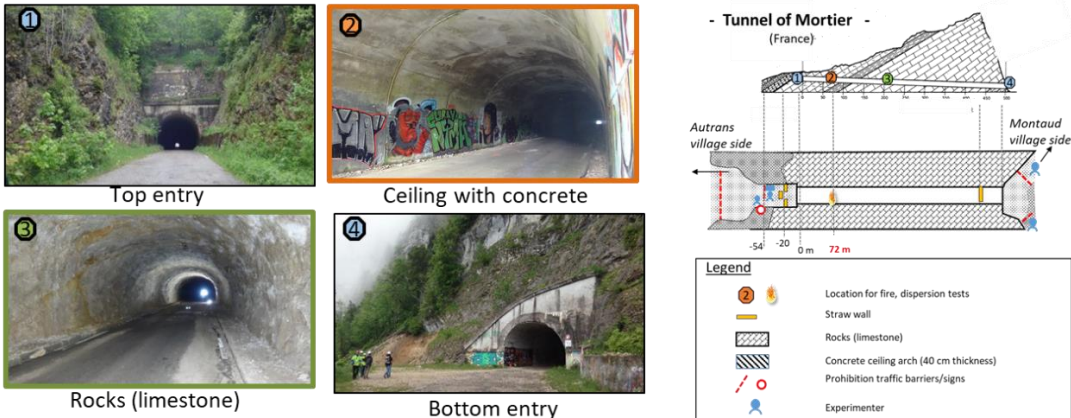


Figure 1. Tunnel geometry

The system used to simulate an HFC-EV vehicle consists of a horizontal plate 4.5m long and 1.9m wide representing the chassis of the car (Figure 2). This chassis is positioned centrally in the tunnel for reasons of symmetry and is 21.5 to 23.5cm above road level (higher curved road on the left side downhill). A type 2 cylinder of about 50 liters at 200 bar represents the tank (B50 tank). The discharge is performed by a Thermally activated Pressure Relief Device (TPRD) located opposite the tank at 15cm from the end of the chassis for safety reasons. This TPRD can be oriented towards the ground or towards the vault. Different diameters have been studied between 0.5 and 3mm. The glass bulb contained in the TPRD was previously broken and the discharge coefficients (C_D) of the orifice were also qualified in dedicated nitrogen experiments. Particular attention has been paid to this injection system to avoid any diameter restriction and to guarantee a very low-pressure drop between the cylinder and the upstream side of the TPRD (the pressure drop is 1×10^{-4} bar with the TPRD of 0.5 mm and 30 bar for the TPRD of 4 mm).

Just upstream of the TPRD, a measuring chamber was installed in order to have the pressure (piezoelectric pressure sensors: Kistler 603CAA, 0-250 bar and Keller PA-23A, 0-200 bar) and temperature of the gas (T-type thermocouple) upstream of the orifice. Then, a stainless steel tube with an internal diameter of 10 mm connects this first measuring chamber with a second one located at the head of the cylinder. The same sensors are installed in this second measuring chamber. Finally, a pneumatic valve with no diameter restriction is located between the two chambers. In the tests, this valve is first closed before fully opening the bottle. In this way, the initial pressure and temperature in the tank are measured. Then the valve is open to start the blow-down test (opening time of 0,7s) and the pressure and temperature transient are recorded.

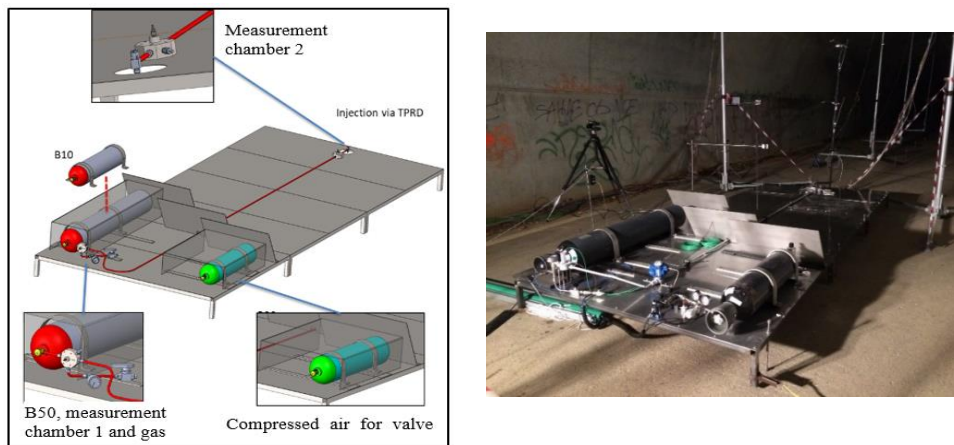


Figure 2. Gas release device

2.2 GAS DISPERSION MEASUREMENT TECHNIQUES

To follow the gas mixture transient, we have positioned eight telescopic masts and four supports to accommodate the various sensors. With pre-calculations, we estimated that a length of +/- 24 m around the discharge is sufficient to capture the different phenomena. To monitor the helium content we use 22 Xensor-Integration XEN-5320 catharometers (accuracy +/- 0.1 vol%). The temperature is measured by about 30 type K thermocouples and by the PT100 contained in the XEN-5320. Oxygen content measurements were also carried out with 20 SGX-40X electrochemical probes from Amphenol Advanced Sensors and a reference zirconia probe (Setnag Liso/F). We also monitor humidity, total pressure and wind speed. The position of the sensors varies according to the test conditions. For vertical upwards releases, the sensors are preferably placed near the top of the vault, whereas for downwards releases, the sensors are more concentrated around and under the chassis. All the experimental data is collected by two acquisition units (NI DAQ 9138 at a frequency of 1Hz and Krypton modules of DeweSoft at a frequency of 20 kHz).

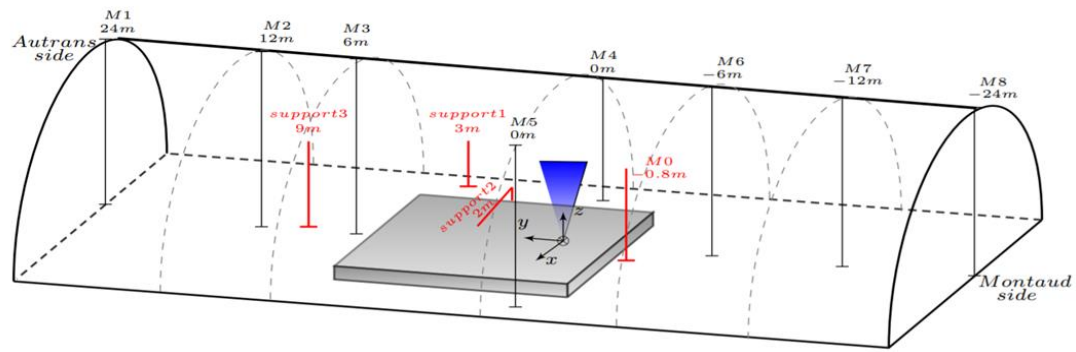


Figure 3. Tunnel representation & masts positions



Figure 4. Gas dispersion measurement sensors

2.3 TEST SEQUENCES

During the tests, the diameter of the TPRD and its orientation were varied as shown in Table 1. The initial conditions in the tunnel before the tests, the duration of the discharge and the total duration of the test are also described. The latter may be slightly longer to follow the helium transport in the tunnel.

Table 1. Dispersion tests sequences.

Test Number	TPRD		Initial conditions			Duration (s)	
	Diameter (mm)	Orientation	Abs Pressure (bar)	Temperature (°C)	RH (%)	Blow-down phase*	Total of test
3	2	Upward	0.854	8.5	92.6	303	437
4	2	Upward	0.837	9.9	88.3	426	582
5**	0.5	Upward	0.837	9.2	96.0	180	181
5***	0.5	Upwards	0.837	6.2	89.82	2650	2657
6	3	Upward	0.837	5.3	88.4	145	249
7	3	Upward	0.844	6.4	75.6	145	165
8	0.5	Downward	0.858	5.4	87.6	2890	3242
9	3	Downward	0.859	5.0	88.9	130	794
10	3	Downward	0.860	5.1	88.2	136	674
11	2	Downward	0.860	6.0	88.7	346	729
12	2	Downward	0.861	6.5	90.2	428	599
13	1	Downward	0.861	7.0	94.2	877	890
14	4	Downward	0.859	7.4	94.9	87	562

* Until 1 bar

** The test was interrupted by a damage in the data acquisition system before the tank was completely empty.

*** The continuation of the test 5 with the end of the same tank

3.0 TEST RESULTS AND ANALYSIS

3.1 TANK BLOW-DOWN TRANSIENT

Measurement of the flow rate at the gas release device (TPRD) was not possible due to the absence of the flowmeter, Hence the flow rate has to be calculated. Two different methods are used to compute the mass flow which are, Mass balance in the bottle and the Sonic nozzle method.

Mass balance in the bottle: In this method, the data of temperature and pressure sensors present close to the TPRD are utilised to determine the density variation (ρ_{gas}). The mass of the gas is computed using the obtained density and the volume of the tank (V_{tank}). The mass flow rate ($Q_{m_{\text{mass balance method}}}$) is computed using the mass balance method for the complete duration of the blowdown period.

$$M_{\text{gas}} = \rho_{\text{gas}} * V_{\text{tank}} \qquad Q_{m_{\text{mass balance method}}} = \frac{\Delta m_{\text{gas}}}{\Delta t}$$

Sonic nozzle method: In this method, the temperature and pressure values from the sensors close to the TPRD are used again. This method uses the theoretical model ‘‘Barré de St Venant’’ to compute the mass flow for a sonic regime, which can be encountered at the exit of the TPRD of the experimental setup. The geometry and the surface quality are not considered in this method and is corrected by introducing the discharge coefficient (C_d).

$$Q_{m_{\text{sonic nozzle method}}} = C_d \cdot S \cdot \sqrt{\gamma \cdot P \cdot \rho \times \left(\frac{2}{\gamma + 1}\right)^{\frac{\gamma + 1}{\gamma - 1}}}$$

The logarithmic scale is considered in the graph shown in figure 5 for a better understanding of the impact of C_d . The mass flow rate reduces more and more as the tank blows down.

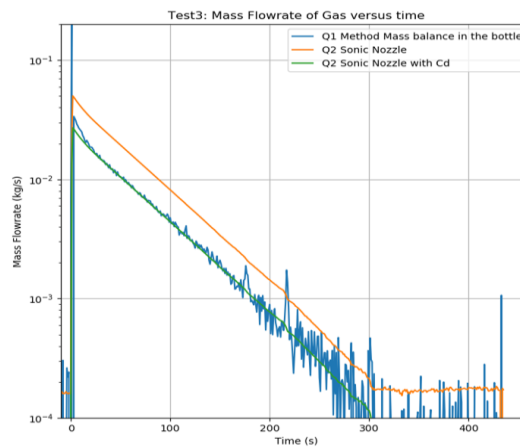


Figure 5. Gas mass flow drop with TPRD of 2mm

The coefficient C_d (represented by green line) is introduced to the sonic nozzle method to fit the mass flow rate to one computed using the mass balance (represented by blue line).

TPRD \varnothing (mm)	0,5	1	2	3
C_d	0.90	0.80	0.62	0.62

The value of C_d obtained from this comparison will be used for other theoretical models. The following table shows some of them.

These C_d values were verified using additional tests carried out on nitrogen at elevated constant pressure in CEA.

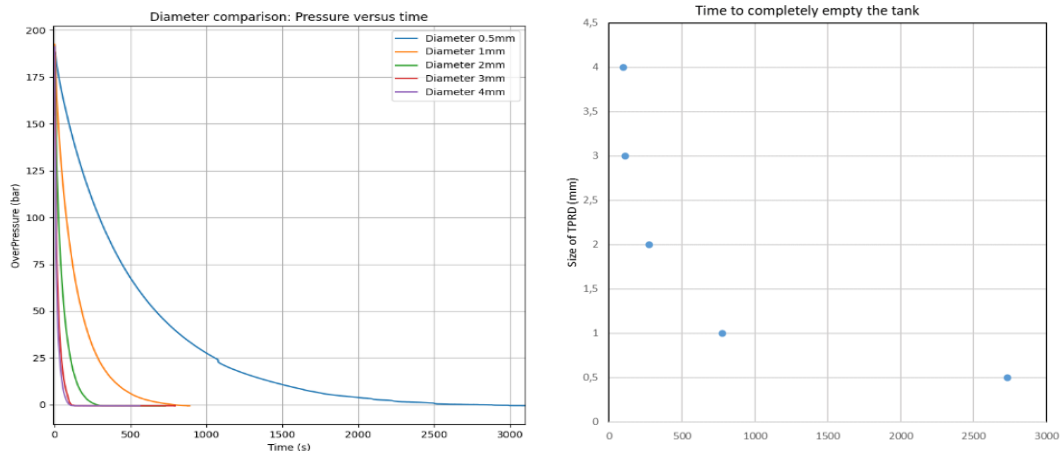


Figure 7. Tank release difference

In figure 6 is observed that the pressure drops decreases gradually as the tank loses gas. This can be realised as the tank with TPRD of 4 or 3 mm gets emptied in less than 2min 30s, while the TPRD of 0.5mm takes more than 41min. These time durations are crucial, as the tank must be able to resist the effect due to fire for this given duration.

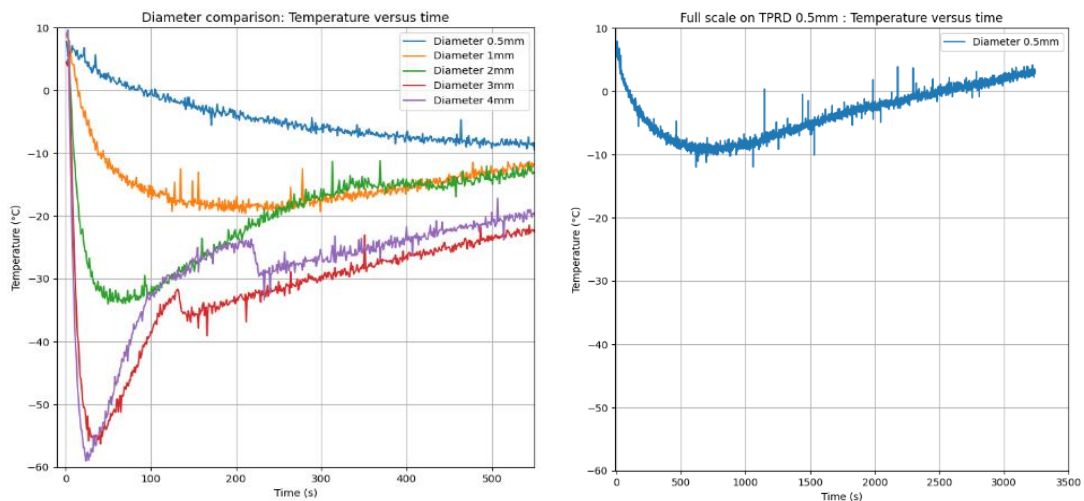


Figure 6. Temperature at the tank's nozzle

The drop in temperature at the orifice of the TPRD (Figure 7) is due to the expansion of the gas, the temperature drops to -58 °C for TPRD of 4mm but for a TPRD of 0.5mm, it does not drop below -10 °C. Gradually the temperature reaches equilibrium before returning to ambient temperature. The delay in reaching the ambient temperature is because the thermal loss due to the expansion of the gas is less significant than the heat input from the outside air.

A slight drop of temperature for the diameter of 3 and 4mm can be observed at the time ~130s and ~220s respectively, this phenomenon appears after the complete emptying of the tank.

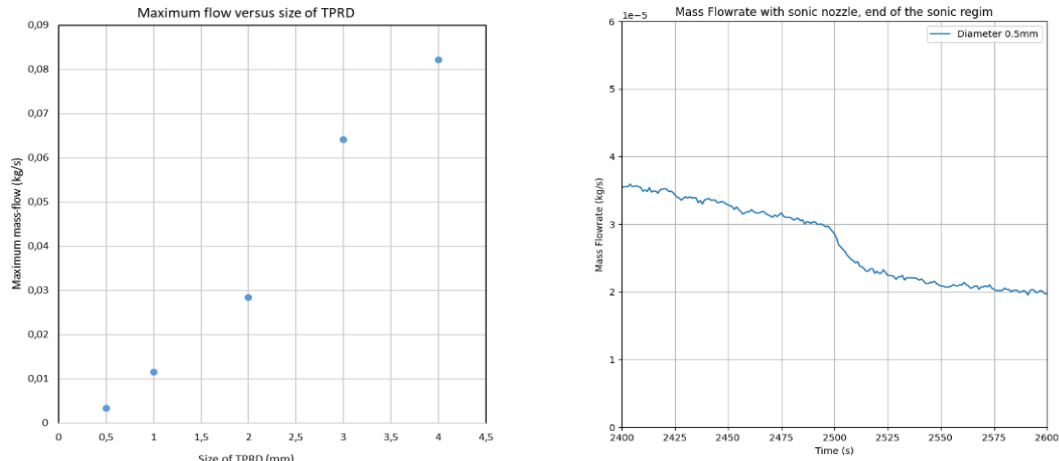


Figure 8. Mass flow

The mass-flow calculated for a real gas (Figure 9) is higher than the mass-flow calculated for an ideal gas, during the initial stage of emptying of the tank (when the pressure is still high). Then the difference in the value decreases so that there is no longer any difference between the two calculation methods. This remark is valid for a depressurization from 200 bar but it will probably be questioned for depressurizations from 700 bar. It can also be observed that the mass-flow at the beginning of the dispersion is higher for large diameter, but drops rapidly.

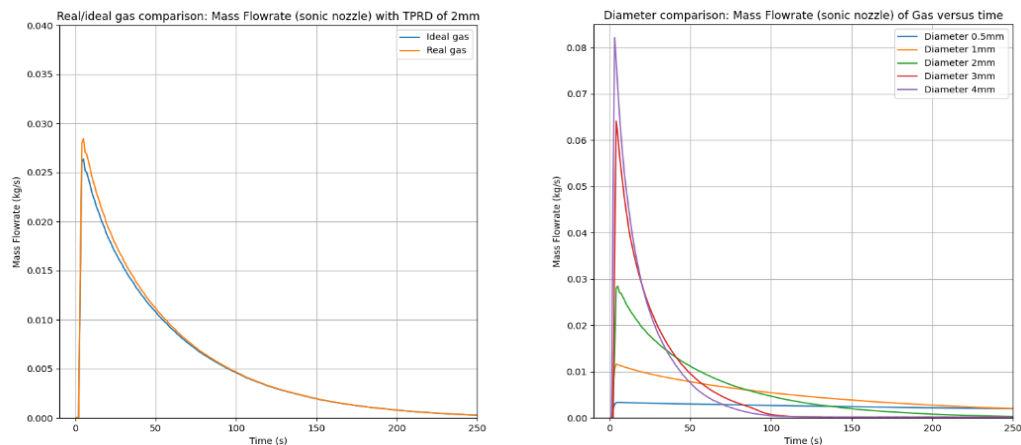


Figure 9. Mass flow conservation

The phenomenon observed on the mass-flow with a TPRD of 0.5mm around 2500s corresponds to the transition from sonic to subsonic regime. These values have been confirmed by some analytical solutions.

3.2 GAS DISPERSION EXPERIMENTS

The analysis of the consequences of a hazardous gas leak is an important part of the risk assessment in the use of hydrogen as an energy vector. This makes essential to know the time-dependent transport of flammable gas from the TPRD outlet of a vehicle during the blowing out of a high-pressure tank.

In the Sandia tunnel safety study [9], the different accident scenarios in which a hydrogen fuel cell electric vehicle (HFCEV) could be involved in a confined space such as a tunnel are mentioned. Here, the cases where the TPRD is activated, but there is no ignition were evaluated, aiming to evaluate the amount of hydrogen that would accumulate in different positions of the tunnel, since the consequences of this event

depend on this amount and the ventilation ratio. During the Sandia study, a probability of 0.02 to 0.85% of such an event is seen.

The concentration percentage is assumed dependent on both, the diameter and the orientation at which the gas is released; these two parameters were evaluated in order to verify the magnitude of influence they have to reach the explosive atmosphere (ATEX). To analyse the influence of the TPRD diameter, various dispersion experiments were conducted with a TPRD of 0.5mm, 1mm, 2mm, 3mm, and 4mm. To study the influence of the orientation, two different scenarios were considered, one where the TPRD is perpendicular to the ground at the chassis' level, pointing towards the tunnel ceiling and the second pointing towards the ground.

The following pictures show the comparison of the measurements of volume concentration for the experiments performed with the TPRD pointing upwards, with a diameter of 0.5mm, 2mm, and 3mm at different points in the tunnel. Figure 10 shows the helium concentration at a distance of 24 meters from the injection point of the TPRD, the image on the left shows the measurement uphill of the tunnel (positive side) on M1 mast, and on the right the measurement on the M8 mast at the same height downhill (negative side). The maximum concentration of 1.2% is observed at this location with the TPRD of 2mm and 3mm.

It can be noticed that, there is not a large variation in the concentration volume between these two diameters and in order to witness a significant reduction in the concentration, the diameter has to be reduced more than 80% in reference to the TPRD of 3mm. Which can be seen in the case of the 0.5mm, where a maximum concentration measured is 0.6% at this distance.

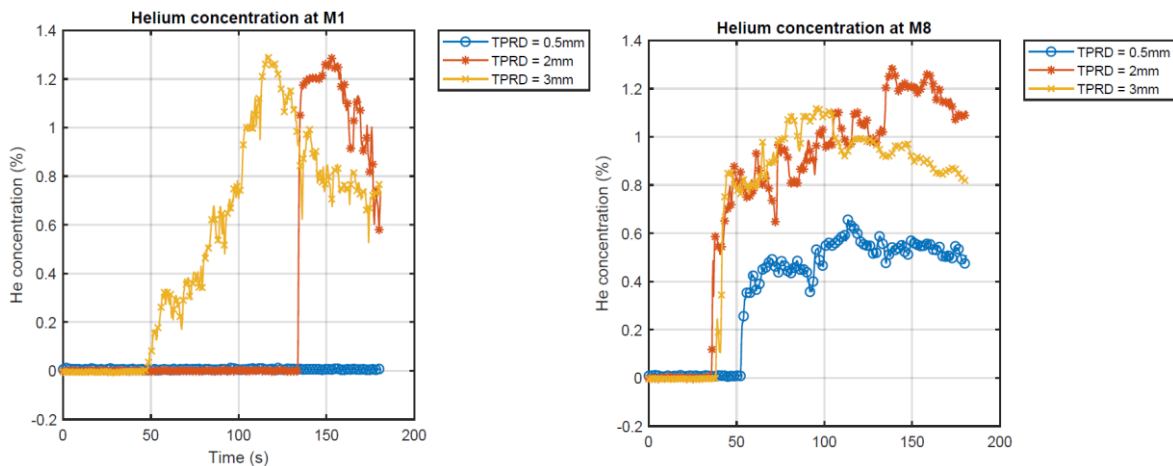


Figure 10. Helium concentration at +/-24m

Shifting closer towards the injection point, at 12m, can be observed in figure 11 a similar behavior as in the previous position, where the 2mm and the 3mm TPRD have a similar concentration measurement, in this case approximately 1.3%. And for the case of 0.5mm a maximum value of 0.7% is obtained. It is possible to observe in these comparisons that the sensors in the downhill of the tunnel receive the helium cloud faster than those in the uphill of the tunnel, even though they are at the same distance. This is due to the direction of the wind, which during most of the experiments was directed towards the lower part of the tunnel.

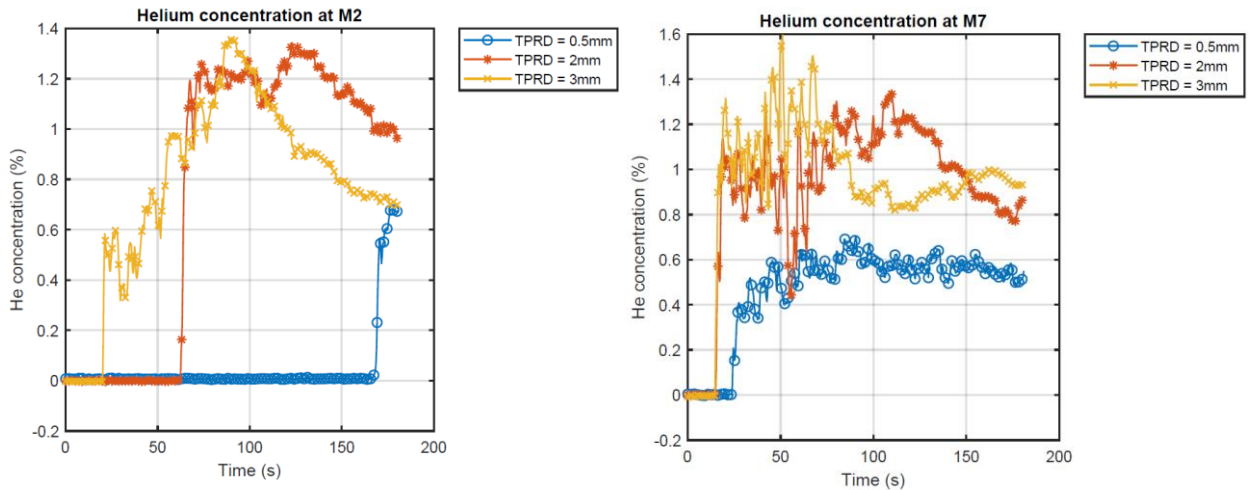


Figure 11. Helium concentration at +/-12m

Finally, on the M3 and M6 masts located six meters from the injection point, a maximum concentration of between 1.6% to 2% was observed for the 2mm and 3mm TPRDs, and a maximum of 0.8% for the 0.5mm one.

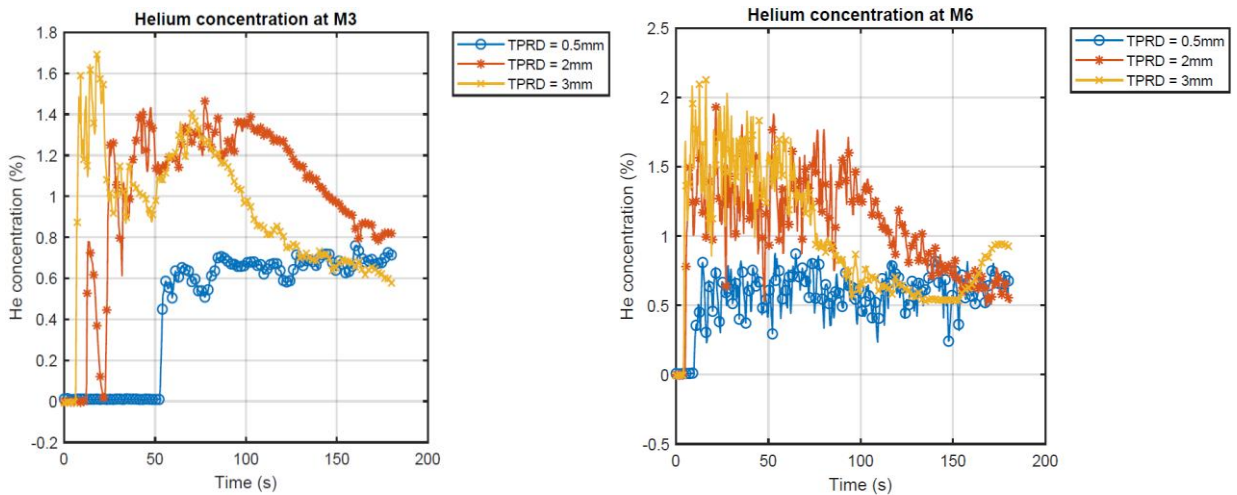


Figure 12. Helium concentration at +/-6m

It is possible to deduce from these experiments that, in none of the cases an explosive atmosphere (ATEX) will be reached and that these values will only be found directly in the jet at the outlet of the TPRD. This is in agreement with the results of the Sandia studies, where it is emphasized that in the case of an opening of the TPRD the hydrogen will be diluted below the ignition limits. The influence of the TPRD diameter is not found to be very significant unless there is a huge reduction in the TPRD.

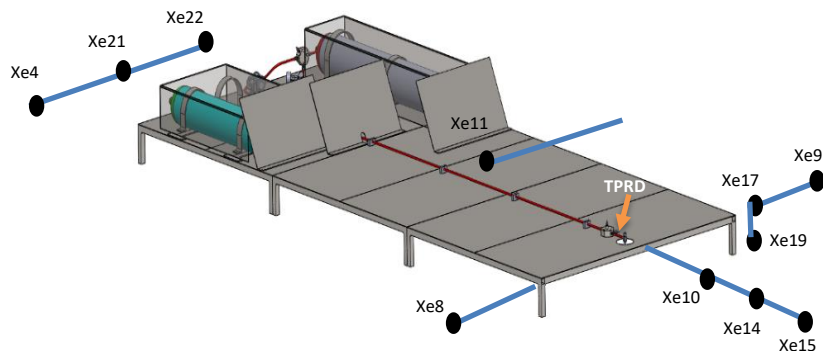


Figure 13. Sensors around the chassis

Following this, to evaluate the influence of orientation, experiments are conducted with the TPRD pointing downwards. In this case, the tip of the TPRD is at a height of approximately 18 cm from the ground and the diameters of 0.5, 1, 2, 3 and 4 mm were evaluated.

For this purpose, 22 catharometers were used, out of which 14 were placed around the chassis at ground level and at chassis height, as shown in the figure 13 below. The rest were still placed on the masts along the tunnel, as in the upward injection case. Initially, the measurements obtained with the 3mm TPRD along the tunnel will be presented, followed by a comparison of the concentration at different points in the tunnel with the different TPRD diameters evaluated.

Figure 14 shows the helium concentration measured at some of the sensors mentioned in the picture above, around the chassis using a 3mm TPRD.

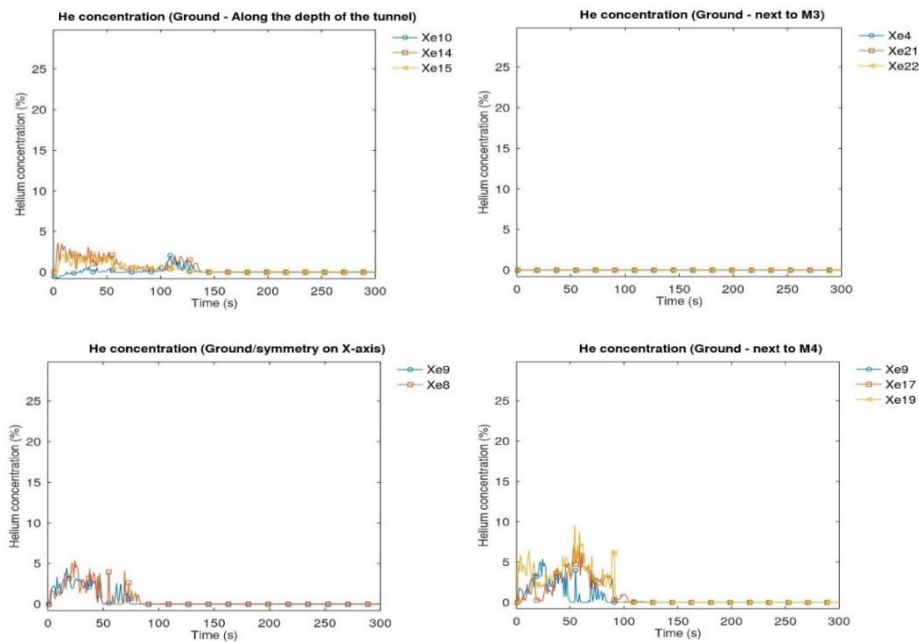


Figure 14. Helium concentration around

The first picture in figure 14 shows a comparison of the measurement on Xe10, Xe14 and Xe15 sensors, located in a structure at the same height as the chassis, along the tunnels length, where no more than 4% concentration is observed. The Xe14 and Xe15 sensors receive the helium cloud faster than Xe10, even though they are further away due to the bouncing of the jet off the ground bypassing around Xe10. On the opposite side of the chassis, three sensors are placed at 6m and at the chassis height, which do not measure any volume concentration during the whole experiment, as shown in the picture on the top right.

Along the positive axis of X, there is a structure with three sensors, two at the height of the chassis and one on the ground. To verify symmetry, sensor Xe8 is located at the same distance as sensor Xe9 but on the opposite side. In this case, no concentrations higher than 5% are observed, except for the Xe19 sensor, which is located at the edge of the chassis and receives the helium cloud coming from below the chassis, measuring almost 9%, this, can be seen in the two lower images of figure 14.

By comparing the different TPRD's diameters, it was observed that, as in the previous case, there is no significant influence of this parameter on the concentration, unless it is decreased to 0.5mm. However, there is a noticeable influence due to the orientation, as there is always the presence of a cloud around and under the chassis with a concentration higher than 4% of the flammability limit of hydrogen, irrespective of TPRD diameters.

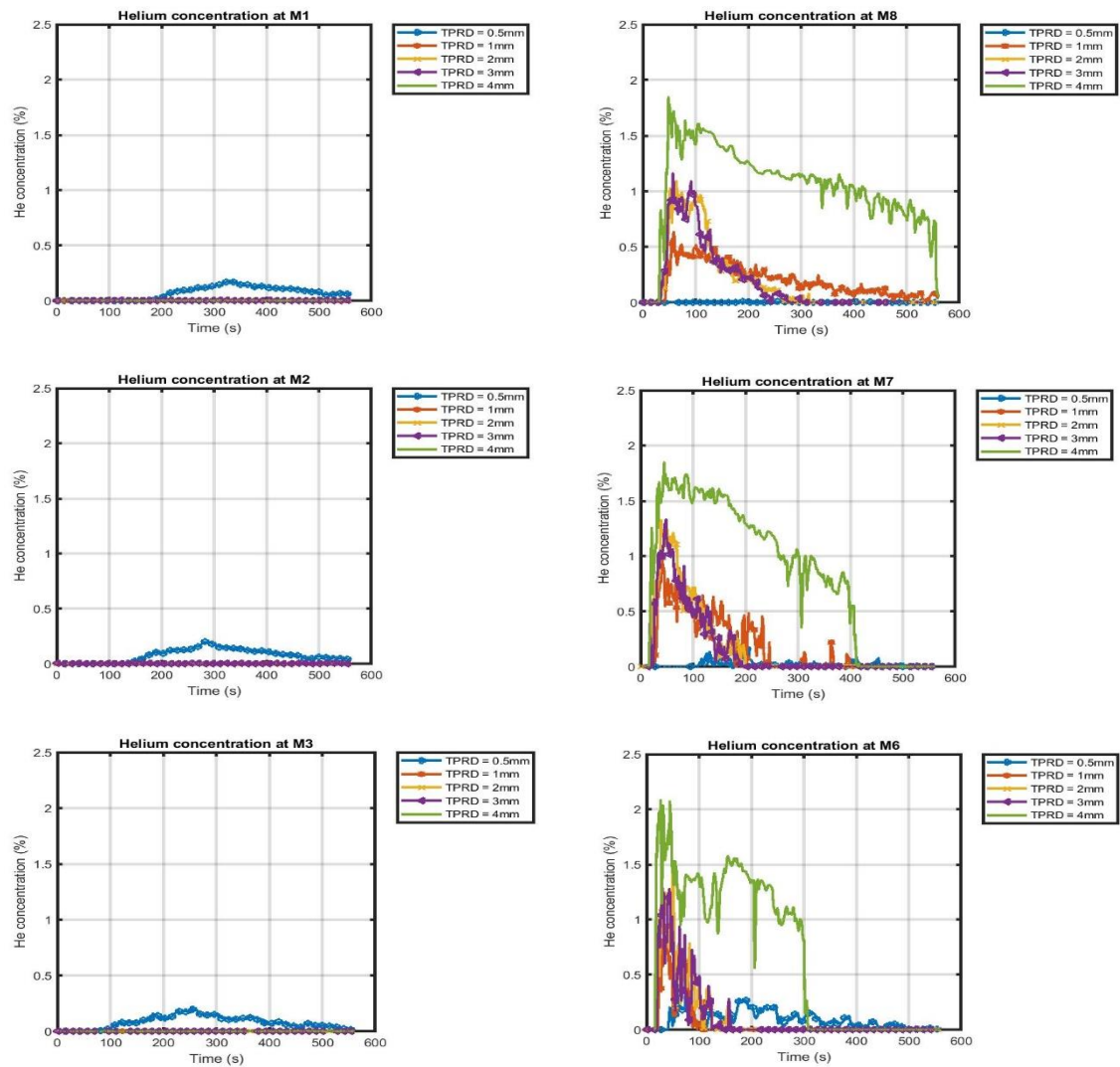
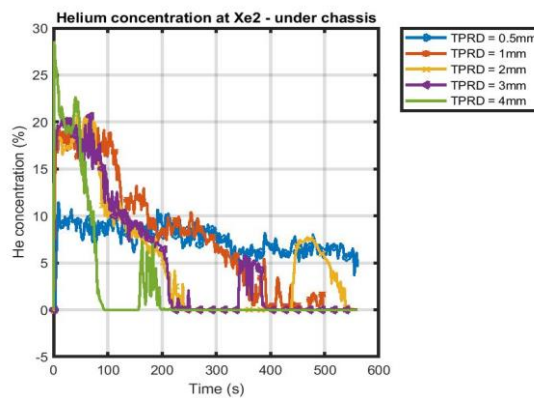


Figure 15. Helium concentration along the tunnel - TPRD of different diameters

The figure 15 above shows all the sensors installed close to the ceiling at different points in the tunnel. The highest concentration is found when using the 4mm TPRD, with a maximum of 1.8% of helium concentration. The TPRD of 1, 2 and 3mm releases approximately the same amount of helium concentration of 1.2%. With a TPRD of 0.5mm, only a maximum of 0.2% is perceived.



The Xe2 sensor measures the helium concentration right under the chassis which is shown in figure 16. It can be seen that with the 4 mm TPRD, the helium volume reaches 28%, and with the 1, 2 and 3 mm TPRD, a helium cloud of between 18 to 23% is measured.

The most favourable case is found with the 0.5 mm TPRD, which reaches a maximum volume concentration of 10%, but remains at this level for a considerable amount of time.

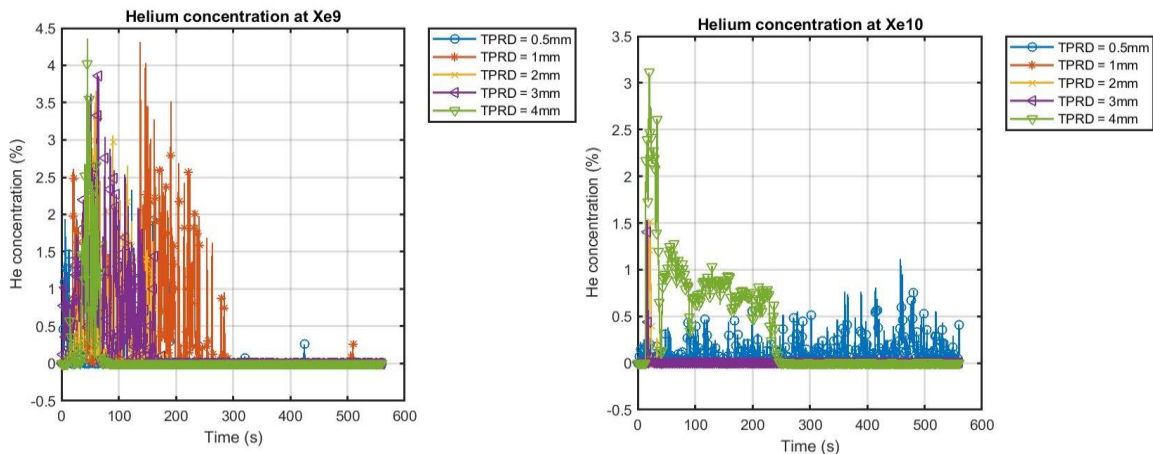


Figure 17. Sensor located around chassis and at chassis height

Around and at the same height of the chassis, a concentration between 3 to 4% is measure for all the TPRDs except for the 0.5mm, which is about 1.5%. There are large fluctuations when it comes to the narrowest axis of the tunnel.

Considering the experiments carried out during the pre-test in Mortier, using a 200 bar helium tank, and the different diameters of TPRDs in different orientations, results can be grouped based on, the concentration measurements close to the ceiling along the tunnel and the ones close to the chassis. In the first case, the values are around 0% to 2% for both upwards and downwards release experiments. The concentration measured around the chassis with the sensors located at chassis height are around 0% to 10%, but the ones under the chassis observed 11% to 28% when the TPRD is oriented downwards.

These results indicate that the area of high risk during a hydrogen release is within 3 meters around the vehicle, if the TPRD is oriented downwards. It must be noted that, at approximately 200s, regardless of the diameter of the TPRD the maximum concentrations would be under the same level, this period can be consider as the critical time during an accident.

4.0 CONCLUSIONS AND PERSPECTIVES

In this paper, we describe the results of preliminary tests, which were conducted in the tunnel du Mortier located in the commune of Autrans in the Vercors, France. Here the dispersion of a non-flammable gas (helium) inside a tunnel was evaluated, in order to verify the maximum concentration value, and the influence of different parameters such as the size and the orientation of the TPRD. From the results obtained, it was possible to verify that the size of the TPRD does not significantly increase the risk, but could reduce the critical time in case of having an adequate natural ventilation (winds between 0.2 and 0.5 m/s).

In terms of orientation, it is observed that the most critical event is when the TPRD is directed downwards, as the whole area around the chassis maintains high levels of gas volume.

It is observed that at lesser than 4 minutes, all measurements with the different TPRD diameters will have approximately the same concentration levels. Within this time duration is when the size of the TPRD really plays a difference in the increment of the magnitude of damages produces in case of ignition. The reduction of this volume in time is directly proportional to the diameter of the TPRD, this leads to further evaluation of the use of a 0.5mm TPRD in different ventilation situations.

This would be the maximum time within which a delayed ignition could be evaluated and thus its maximum severity level in case of occurrence. Taking into account that experiments by Schefer et al. [10] show that ignition of a turbulent hydrogen jet requires 8% concentration to achieve ignition instead of 4% concentration seen in stagnant mixtures.

However, a delayed ignition scenario is not the most likely, as ignition of the flammable gas will normally occur almost instantaneously. Since, if the TPRD is activated, it is due to a high temperature, which will normally result in a jet fire, and not a deflagration due to a pre-mixing of hydrogen and air, which would result in an overpressure [1].

In conclusion, there is no significant influence of the diameter of the TPRD but the orientation of the TPRD does have an influence. To reduce the ATEX generated under the chassis, it will be desirable not to use it completely perpendicular to the ground and as close as possible to the edge of the chassis to avoid accumulation under the chassis.

During the second campaign, while evaluating a 70MPa release, it will be important to evaluate the concentration over a longer period in order to better observe the critical time when using each size of TPRD.

REFERENCES

- [1] W. G. Houf, G. H. Evans, E. Merilo, M. Groethe, and S. C. James, "Releases from hydrogen fuel-cell vehicles in tunnels," *11th China Hydrog. Energy Conf.*, vol. 37, no. 1, pp. 715–719, Jan. 2012, doi: 10.1016/j.ijhydene.2011.09.110.
- [2] Y. Sato *et al.*, "Hydrogen Release Deflagrations in a Sub-Scale Vehicle Tunnel," presented at the World Hydrogen Energy Conference WHEC 16, Lyon, France, 2006.
- [3] A. G. Venetsanos, D. Baraldi, P. Adams, P. S. Heggem, and H. Wilkening, "CFD modelling of hydrogen release, dispersion and combustion for automotive scenarios," *Hydrog. Saf.*, vol. 21, no. 2, pp. 162–184, Mar. 2008, doi: 10.1016/j.jlp.2007.06.016.
- [4] P. Middha and O. R. Hansen, "CFD simulation study to investigate the risk from hydrogen vehicles in tunnels," *2nd Int. Conf. Hydrog. Saf.*, vol. 34, no. 14, pp. 5875–5886, Jul. 2009, doi: 10.1016/j.ijhydene.2009.02.004.
- [5] H. Y. Bie and Z. R. Hao, "Simulation analysis on the risk of hydrogen releases and combustion in subsea tunnels," *Spec. Issue 6th Int. Conf. Hydrog. Saf. ICHS 2015 19-21 Oct. 2015 Yokohama Jpn.*, vol. 42, no. 11, pp. 7617–7624, Mar. 2017, doi: 10.1016/j.ijhydene.2016.05.263.
- [6] Y. Li *et al.*, "Numerical analysis of hydrogen release, dispersion and combustion in a tunnel with fuel cell vehicles using all-speed CFD code GASFLOW-MPI," *Int. J. Hydrog. Energy*, Oct. 2020, doi: 10.1016/j.ijhydene.2020.09.063.
- [7] J. He, E. Kokgil, L. (Leon) Wang, and H. D. Ng, "Assessment of similarity relations using helium for prediction of hydrogen dispersion and safety in an enclosure," *Int. J. Hydrogen Energy*, vol. 41, no. 34, pp. 15388–15398, Sep. 2016.
- [8] A. Prabhakar, N. Agrawal, V. Raghavan, and S. K. Das, "Numerical modelling of isothermal release and distribution of helium and hydrogen gases inside the AIHMS cylindrical enclosure," *Int. J. Hydrogen Energy*, vol. 42, no. 22, pp. 15435–15447, Jun. 2017.
- [9] C. LaFleur, G. Bran-Anleu, A. Muna, B. Ehrhart, M. Blaylock and W. Houf, "Hydrogen fuel cell electric vehicle: Tunnel safety study", *Sandia Report*, SAND2017-11157, Sandia national laboratories.
- [10] R. Schefer, G. Evans, J. Zhang, A. Ruggles, and R. Greif, "Ignitability limits for combustion of unintended hydrogen releases: experimental and theoretical results" *Int. J. Hydrogen Energy*, vol. 36, no. 3, pp. 2426-2435, 2011.